Seismic behavior of high-performance fiber reinforced composite frames

Vojko Kilar[1] and N. Krstulovič-Opara[2]

ABSTRACT | The paper explores the possibilities to use a High-Performance Fiber Reinforced Concretes (HPFRCs) for design of seismic resistant cost-effective and durable buildings. Composite frame buildings are made through selective use of different HPFRCs: Slurry Infiltrated Mat Concrete (SIMCON), Slurry Infiltrated Fiber Concrete (SIFCON) and High Strength - Lightweight Aggregate Fiber Reinforced Concrete (HS-LWA FRC) which further minimizes dead and seismic loads. The first part of the paper briefly describes used HPFRCs and proposed composite building system consisted of composite columns, beams and specially designed fuses that connect the two. In the second part of the paper the results of the nonlinear static analysis of an isolated composite beam as well as of the nonlinear dynamic analysis of a whole four-story example composite building are presented. The response in terms of force-displacement relationships and rotational ductility factors as well as in terms of base shear, top displacements and global damage index histories is compared to the response of an identical classical four-story building made of reinforced concrete.

KEYWORDS | Fiber Reinforced Concrete, High Performance Fiber Reinforced Concrete, Composite Building Structures, Seismic behavior, Frame Structures, Nonlinear analysis

1 Introduction

Major progress has been made in recent decades in the development of Fiber Reinforced Concrete (FRC), and High-Performance FRC (HPFRC). Conventional FRCs are made by premixing discontinuous fibers with concrete in which case due to workability requirements the maximum fiber volume fraction of steel fibers is limited to approximately 2%. At such a low volume fraction fibers mainly contribute to post-cracking ductility and energy absorption [1]. HPFRCs are a newer class of FRCs which exhibits behavior particularly desirable for earthquake-resistant design: significantly increased strength, ductility and energy absorption [2,3]. HPFRCs used in the presented research include: (a) SIMCON [4-7], and (b) SIFCON [2,8]. Both are manufactured by pre-placing fibers into the form, followed by infiltration of a specially designed high strength cement-based. The key difference between the two is that SIMCON is made with continuous fiber-mats, while SIFCON is made with high fiber volume fractions of discontinuous fibers. Since fiber orientation in SIMCON fiber-mats can be controlled, very high tensile strengths and ductilities are reached for a comparatively low fiber volume which translates into high improvement in structural response [6,9]. However, due to its fiber-mat configuration, SIMCON is not well suited for manufacturing of "fuses," in which case SIFCON is a better alternative [10].

1. University of Ljubljana, Faculty of Civil and Geodetic Engineering, IKPIR, Jamova 2, 1000 Ljubljana, Slovenia, Email: vkilar@ikpir.fagg.uni-lj.si
2. Exponent Failure Analysis Associates, 149 Commonwealth Drive, Menlo Park, CA 94025, USA, Email nkrstulovic@exponent.com

Previous use of two particular HPFRCs: Slurry Infiltrated Fiber Concrete (SIFCON) and Slurry Infiltrated Mat Concrete (SIMCON) in seismic retrofit resulted in large increases in ductility, strength and energy dissipation of the otherwise non-ductile beam-column subassemblages [11,12]. Successful worldwide use of conventional FRCs has demonstrated that fibers can replace stirrups and ties, resulting in higher shear and flexural strength, higher stiffness and slower stiffness degradation, higher ductility and energy dissipation, better concrete confinement and better re-bar bond, leading to substantially better, safer and more economical seismic-resistant performance over conventional reinforced concretes.

The purpose of the presented research was to reconsider existing procedures for design and construction of R.C. frames, and develop an alternative approach better suited for cost -effective, seismically resistant use of HPFRCs. Such a frame, termed herein High-Performance Composite Frame (HPCF), is made by selectively using: High Strength - Lightweight Aggregate FRC (HS-LWA FRC), Slurry Infiltrated Mat Concrete (SIMCON) and Slurry Infiltrated Fiber Concrete (SIFCON). The proposed HPCF consists of three main elements: (1) a composite beam member made with a precast SIMCON "jacket" and cast-in-place HS-LWA FRC core, (2) a composite HS-LWA FRC filled steel tube column member, and (3) a precast SIFCON "fuse" connecting the two, as shown in Figures 1, 2 and 3.

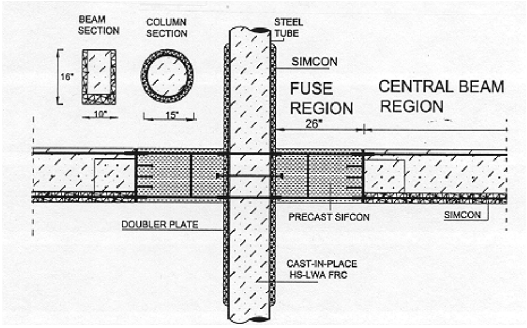

Figure 1. Layout of a HPCF beam; beam – column connection.

Figure 2. The 2.5 cm (1 in.) thick 1.52 m (5 ft) long, 40.6 cm (16 in.) high and 25.4 cm (10in.) wide SIMCON stay-in-place formwork. Shear studs that were bolted directly into the formwork sides are clearly visible.

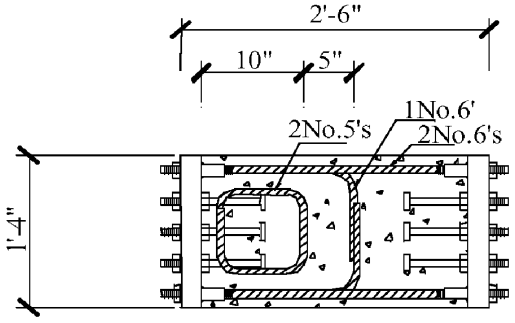

Figure 3. Layout of a representative SIFCON fuse specimen.

2 Results of experiments and data for nonlinear analyses

This section summarizes experimentally determined member response of fuses, beams and columns. The tests were performed on North Carolina State University by second author and his co-workers. Deformation of tested specimens along the specimen height were measured by a series of strain gages, potentiometers, and clinometers. Only the test results that were used to

determine the analytical models for beams, fuses and columns (e.g. measured moment-curvature responses) are presented within this paper. The list of references with more detailed description of tests and material properties of HPCF members can be find in [7,9,11 and 13].

2.1 Beam member

No conventional reinforcement was used in 40.6 cm (16 in.) high and 2.5 cm (1 in.) thick formwork walls of tested beam. Use of SIMCON eliminated the need for stirrups, while its high strength and toughness permitted direct bolting of shear studs and connection bolts into the formwork walls, as shown in Figure 2. The section "core" was cast-in-place, 2% fiber volume fraction, 80.7 Mpa (11,700 psi) HS-LWA FRC, with the unit weight of 19.6 kN/m^3 (123 lb/ft^3). The beam specimen was tested under cantilever-type reverse cyclic loading. Moment-curvature response of beam member is presented in Figure 4.

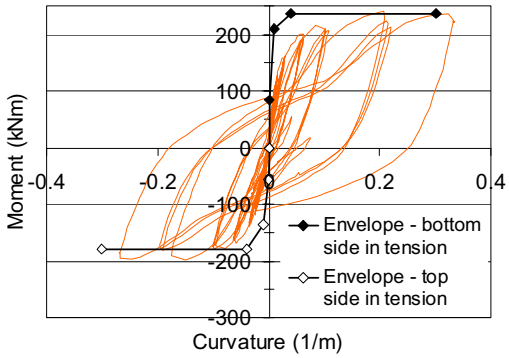

Figure 4. Test response of SIMCON/HS-LWA FRC beam member under reversed cyclic loading and corresponding moment-curvature envelopes.

2.2 Fuse member

Fuse member provides an energy “sink” under severe seismic excitations by forming a plastic hinge [14]. To both increase the construction speed and simplify replacement of damaged fuses after an earthquake, precast “fuses” were developed (Figure 3). The effect of reinforcement layout and SIFCON properties on fuse behavior was evaluated and optimized [15]. In the present research it was anticipated that the fuses should be replaceable after the damage occurred, so the yielding of the interface sections should be eliminated or minimized. This goal was successfully achieved and the main source of energy absorption was the zone in the middle of the fuse. Moment-curvature response of fuse member is presented in Figure 5.

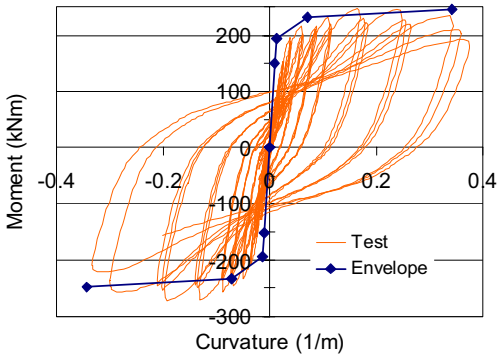

Figure 5. Test response of fuse member under reversed cyclic loading and corresponding moment-curvature envelopes.

2.3 Column member

If adequately confined, HS-LWA concrete is ideally suited for column members [16]. To maximize con-

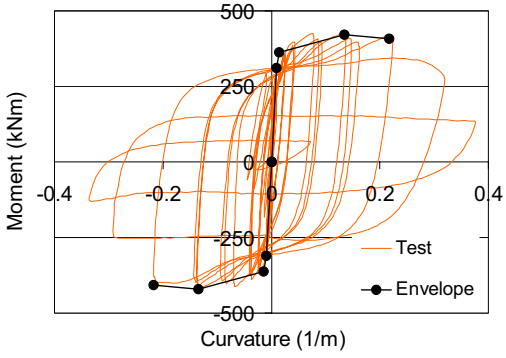

Figure 6. Test response of column member under reversed cyclic loading and corresponding moment-curvature envelopes.

finement HS-LWA FRC was encased in a steel tube, as shown in Figure 1. Under a static -reversed cyclic loading specimen exhibited stable response, hysteretic loops were wide and a specimen failure initiated by the "elephant foot" buckling of the steel tube, followed by formation of steel cracks which led to the final failure of the specimen. Moment-curvature response of fuse member is presented in Figure 6.

2.4 Dimensions and scaling

The main goal of analytical investigation was to compare the response of HPCF building with the response of conventional RC frame building. The selected reference R.C. (i.e., "Ispra") structure, shown in Figure 11, was designed in accordance with the seismic requirements of the Eurocode 2 and 8 for High Ductility structures and was tested under pseudodynamic loading in the European Laboratory for Structural Assessment in Ispra in Italy [17]. The same building dimensions and the same cross section dimensions were used also for HPCF building. Thus, the tested HPCF beam, fuse and column cross-sectional dimensions were scaled up to Ispra dimensions (scale factor 1/0.84 was used), while the column diameter was scaled to 0.386 m (15.2 in). Experimentally obtained member properties were scaled up following the "true model" scaling laws [18]. Resulting final cross-sectional dimension of both the fuse and the model central beam region were 30 cm x 48.6 cm (11.9 in. x 19 in.). While the center-to-center column spacing of 5 m was the same as for the reference Ispra building, scaled SIFCON fuse length was 78.6 cm (30.9 in.). Resulting elastic moduli of the SIMCON beam member, fuse and column were equal to $Eb = 4.15 \cdot 10^7$ kN/m^2 ($6.02 \cdot 10^6$ psi), $Ef = 1.16 \cdot 10^7$ kN/m^2 ($1.68 \cdot 10^6$ psi), and $Ec = 5.78 \cdot 10^7$ kN/m^2 ($8.38 \cdot 10^6$ psi), respectively. The characteristical points of envelopes scaled for dimensions of Ispra building and used for nonlinear analysis with computer program CANNY/E [19] (estimated crack, yield and ultimate points for Takeda nonlinear model) are presented in Table 1.

3 Analysis of an isolated high performance composite beam

The nonlinear analysis of an isolated HPC beam was carried out first. The purpose of the analysis was to determine the fuse/beam length ratio and fuse/beam strength ratio in a way that fuses at the end of beam can protect the central part of beam from damage. Obtained results will be used for the nonlinear dynamic analysis of entire HPFRC-based composite-frame system presented in the next chapter.

3.1 Model description

The analyzed beam is taken out from a frame and it is positioned vertically and fixed at both ends (Figure 7). The model simulates a beam in a frame subjected to strong horizontal loading. The force is introduced at the top and increased up to the point when top displacement reaches 2% of beam length L (this value

Table 1. Characteristical points of moment-curvature envelope for nonlinear analysis of HPCF members (scaled values for Ispra dimensions)

	Fuse		Beam (Bottom in tension)		Beam (Top in tension)		Column	
	Curvature (1/m)	Moment (kNm)	Curvature (1/m)	Moment (kNm)	Curvature (1/m)	Moment (kNm)	Curvature (1/m)	Moment (kNm)
Crack	0.008	255	0.001	142	0.001	95	0.008	524
Yield	0.038	389	0.019	399	0.021	301	0.022	650
Ultimate	0.288	416	0.252	399	0.252	301	0.18	690

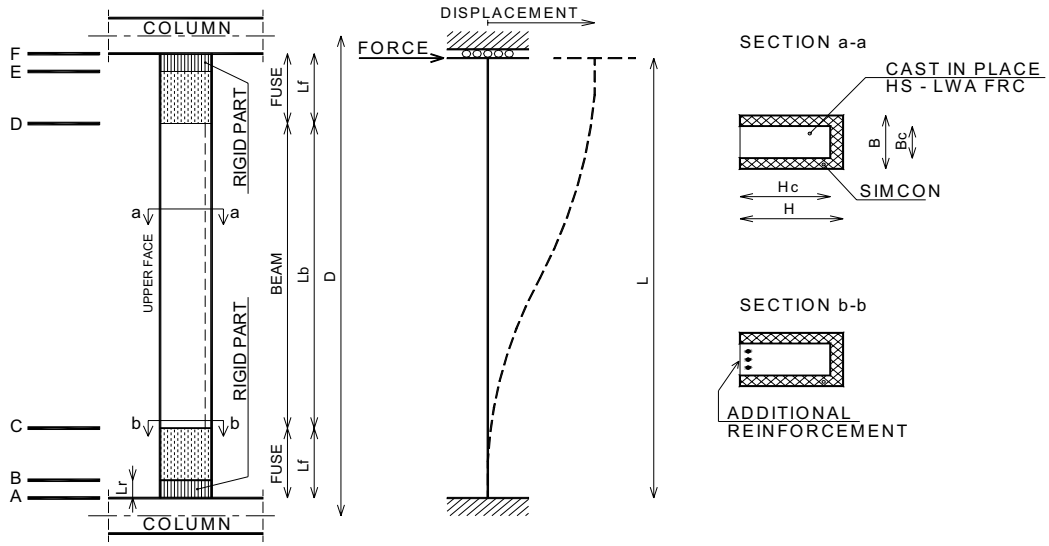

Figure 7. Mathematical model for the analysis of isolated beam.

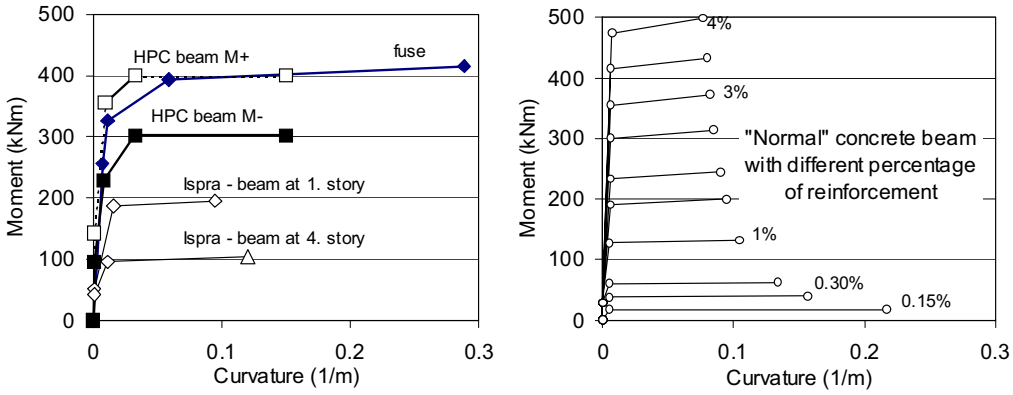

Figure 8. Comparison of moment curvature relationship for HPC and Ispra beams as well as for "normal" concrete beams with different percentage of reinforcement (symmetrically positioned reinforcement, top=bottom, C25/30).

corresponds to life safety performance level for RC beams). Fuses are located at the both sides of the beam. The effect of vertical loading has been neglected. The analyzed HPC beam has the following dimensions: D=5.0 m, L=4.6 m, L_f=0.786 m, L_b=3.028 m L_r=0.2 m, H=0.483 m, H_c=0.423 m, B=0.3 m and B_c=0.242 m. In the mathematical model the length of fuse up to 0.20 m away from column face was considered as rigid.

3.2 Comparison of moment-curvature relationships

Figure 8 presents the comparison of moment curvature relationships for HPC and Ispra beams. It can be seen from Figure 8 that HPC beams have considerably higher strength as RC beams used in Ispra building. It can be also seen that the HPC beams have approximately the same strength as the normal concrete beam

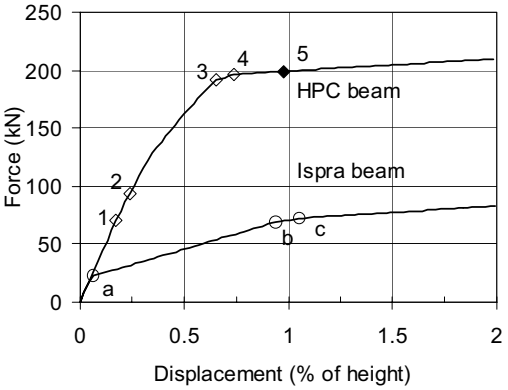

Figure 9. Force-displacement relationship for HPC and Ispra beam.

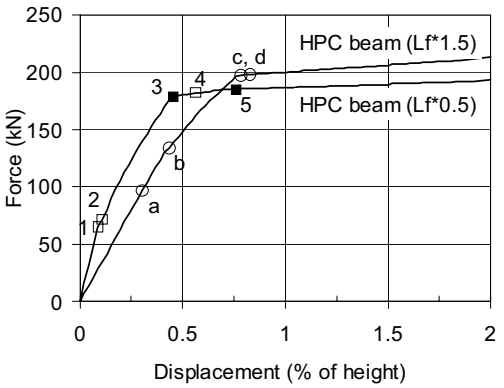

Figure 10. Force-displacement relationship for HPC beams with different fuse length.

with 3% of reinforcement. HPC beams have higher curvature ductilities as corresponding RC beams. It can be also seen from Figure 8 that the fuse has approximately the same strength as HPC beam, but it has considerably higher ductility which is necessary to absorb energy in order to protect the central part of HPC beam from damage.

3.3 Results of nonlinear static analysis of isolated beam

Figure 9 presents the force-top displacement relationship for analyzed HPC beam. As a comparison the same relationship obtained for the strongest beam from Ispra building is also presented. Figure 10 presents the same relationship for the cases of half longer and half shorter fuses. It can be seen from Figure 9, that the HPC beam has considerably higher strength than Ispra beam and thus provides better resistance during earthquake excitations. The change in fuse length (Figure 10) affects mostly the initial stiffness (shorter the fuse bigger the stiffness), but the final strength does not change significantly. In table 2 the spread of damage is recorded for all investigated variants.

With close observation of spread of damage we can observe that in the analyzed HPC beam and in the HPC beam with reduced length, the fuses do not protect the beam when bigger displacements are reached (see point 5 in Figure 9 and points 3 and 5 in Figure 10 as well as Table 2). The beam protection is even less effective if the fuse is shorter. In these cases the beams yield before the fuses do. The yielding of beam occurs at the upper face of the beam (Figure 7, section C), where due to required U shape of SIMCON concrete formwork the resistance of a beam is reduced. However, in the case of increased length of the fuse, the yielding of beam was not recorded. In this case the cracking occurred first at the top and the bottom of beam, and after, as required, the fuses yield at the both ends. The further increase of displacement did not cause the yielding in the central part of the beam. Instead of increasing the fuse length, the problem can be solved also with adding an additional reinforcement at the upper face of the beam (see section b-b in the Figure 7, where three bars Φ14 were added). The favorable spread of damage for the case with additional reinforcement is also presented in the Table 2. For further studies presented in this paper the fuses with length 0.786 m (length of fuse is approx. 15% of length of beam) with additional top reinforcement bars will be used.

Table 3 presents the rotation ductility factors for Ispra beam and for all investigated variants with different fuse lengths. The ductility factors are determined for the beam top displacement equal to 2% of beam length. It can be seen that only the HPC beam with

Table 2. Spread of damage in HPC and RC beams (values in brackets apply for HPC beam with additional reinforcement at the top).

HPC beam			Ispra beam		
Event	**Description**	**Top displ. (%L)**	**Event**	**Description**	**Top displ. (%L)**
1	Cracking of beam (section C)	0.17 (0.17)	**a**	Cracking (sections A and F)	0.07
2	Cracking of beam (section D)	0.24 (0.24)	**b**	Yielding (section F)	0.94
3	Yielding of fuse (section E)	0.65 (0.65)	**c**	Yielding (section A)	1.07
4	Yielding of fuse (section B)	0.74 (0.74)	/	/	/
5	Yielding of beam (section C)	**1.04 (3.52)**	/	/	/

HPC beam (L_{fuse}*0.5)			HPC beam (L_{fuse}*1.5)		
Event	**Description**	**Top displ. (%L)**	**Event**	**Description**	**Top displ. (%L)**
1	Cracking of beam (section C)	0.11	**a**	Cracking of beam (section C)	0.30
2	Cracking of beam (section D)	0.13	**b**	Cracking of beam (section D)	0.43
3	Yielding of beam (section C)	**0.48**	**c**	Yielding of fuse (section E)	0.78
4	Yielding of fuse (section E)	0.56	**d**	Yielding of fuse (section B)	0.80
5	Yielding of beam (section D)	**0.73**		/	/

Table 3. Ductility factors* at 2% top displacement.

Cross section	HPC beam	HPC beam with add. reinf.	Ispra	HPC beam (Lf*0.5)	HPC beam (Lf*1.5)
A	/	/	6.2 beam	/	/
B	6.4 fuse	8.4 fuse	< 1	< 1	8.0 fuse
C	**6.2 beam**	< 1	< 1	**10.6 beam**	< 1
D	< 1	< 1	< 1	**8.5 beam**	< 1
E	9.3 fuse	9.1 fuse	< 1	10.4 fuse	8.4 fuse
F	/	/	7.1 beam	/	/

* Ductility factor is defined as a ratio between yield rotation and ultimate rotation reached at the displacement 2%L.

additional reinforcement and HPC beam with increased length can successfully protect the central part of beam also for the cases of larger displacements. It can be noted that the ductility factors in both mentioned cases are slightly bigger than for the Ispra beam. This is the consequence of the fact that the fuses, due to their special design, yield at smaller displacement as the Ispra beams do. Since the fuses are specially designed to accommodate bigger damage the allowa-

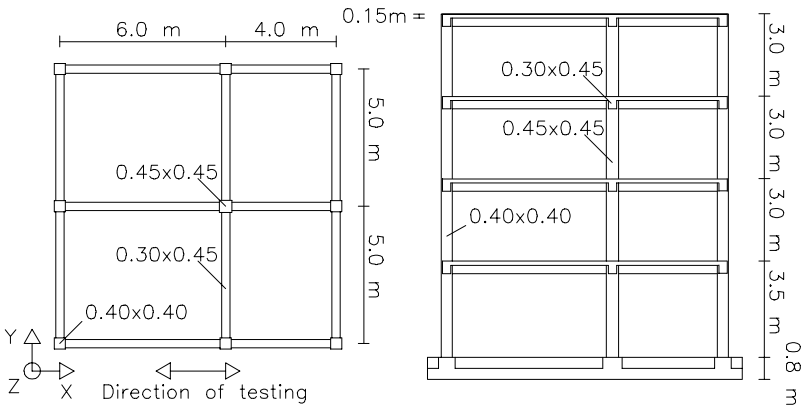

Figure 11. Reference test building from Ispra [17].

ble rotational ductility factor is bigger as for regular RC beams as shown for example in [14] and [15].

4 Analysis of a high performance composite frame building

4.1 Description of a reference Ispra building

The reference test structure [17] is a four-story R/C frame building (Figure 11) designed in accordance with the prescriptions of Eurocode 2 and 8 for High Ductility class structures. Dimensions in plan are 10 m x 10 m; interstory heights are 3.0 m, except for the ground story which is 3.5 m high. The structure was symmetric in the direction of testing (X direction), with two spans equal to 6.0 and 4.0 m. All columns have square cross section with 400 mm side, except for the interior column which is 450 mm x 450 mm; all beams have rectangular cross section, with total height of 450 mm and width of 300 mm. A solid slab, with thickness of 150 mm, was adopted for all stories of Ispra building. In the pre-liminary design of the building additional dead load to represent floor finishing and partitions equal to 2.0 kN/m^2, live load equal to 2.0 kN/m^2, peak ground acceleration of 0.3g, soil type B, importance factor equal to 1 and behavior factor q equal to 5 were assumed. The seismic input was an artificial accelerogram, called S7, generated by using the waveforms derived from real signals recorded during the 1976 Friuli earthquake: its response spectrum fits the one given by EC8 for soil profile B at 5% damping. High and low level pseudo dynamic tests were performed in the European Laboratory for Structural Assessment (ELSA), using such accelerogram S7 scaled by 1.5 and 0.4 respectively. In our study the Ispra and HPCF buildings were subjected to S7 accelerogram scaled by factor 1.5. The HPCF building was subjected also to S7 accelerogram scaled by factor 2.0. The loading was oriented in X direction only. The artificial accelerogram and corresponding response spectra are presented in Figure 12.

4.2 Numerical modeling

The model was set up using all the available theoretical and experimental data. CANNY-E computer program [19] was used to perform the static and dynamic numerical analyses. For Ispra building the geometry of the modeled building and the masses, concentrated in the center of mass of each floor, are taken from [17]. The building is modeled as a planar structure consisted of three parallel frames. The damping matrix is assumed to be proportional to the instantaneous stiffness matrix, assigning a damping ratio equal to 2%.

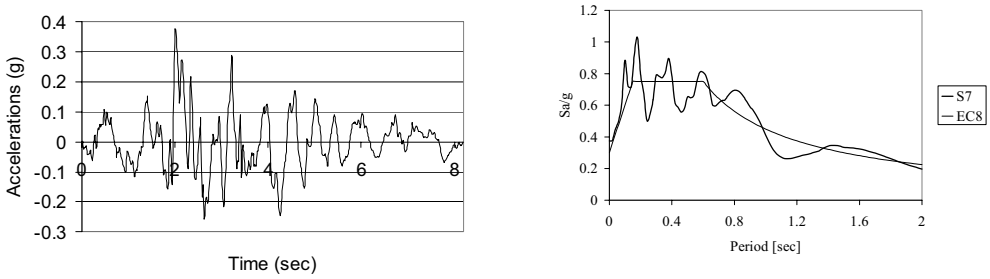

Figure 12. Artificial accelerogram S7 and Eurocode 8 and S7 elastic spectra.

Table 4. Periods for Ispra and HPCF building before and after dynamic step-by-step analysis.

	Ispra (sec)		HPCF building (sec)		
	Elastic	After nonlinear dynamic analysis (S7*1.5)	Elastic	After nonlinear dynamic analysis (S7*1.5)	After nonlinear dynamic analysis (S7*2.0)
X1	0.56	1.24	0.55	0.60	0.67
X2	0.18	0.36	0.17	0.18	0.19
X3	0.10	0.20	0.09	0.10	0.10

The beams are idealized by a nonlinear uni-axial bending model, the inelastic flexural deformations are lumped at the element ends and described by the rotation of two nonlinear springs, which are connected to the joint by a rigid zone. The moment-rotation relationships in the two rotational springs are computed based on moment-curvature relationships (Table 1), assuming an asymmetrical moment distribution along the length of the element. A tri-linear skeleton curve is assigned to represent the cross section behavior before and after cracking and yielding. The hysteretic behavior follows the Takeda rules, but the pinching effect is also considered. Best correlation with the experimental results for Ispra building was obtained assuming small values for the unloading stiffness (in each cycle it is reduced of 50% with respect to the previous one). The columns are idealized with the same nonlinear uni-axial bending model as it is used for the beams. A detailed study of the influence of different model parameters to the response of Ispra building can be found in [20].

It the present phase, the same model assumptions were used also to model a new HPCF building. The beams were divided in to two fuse elements and one central beam element. The total calculated mass is approximately 10% smaller than for Ispra building, due to light-weight concrete used for beams of new building. The contribution of floor slabs was not taken into account as it was for Ispra building. Table 4 presents the periods for both investigated buildings obtained before and after step-by-step analysis. It can be seen that periods for HPCF building are slightly smaller than for Ispra building; the differences are bigger after the building is already damaged. The reason is mainly due to smaller masses and slower stiffness deterioration of HPCF building.

4.3 Results of nonlinear dynamic analysis

This chapter presents the results of nonlinear dynamic analysis of Ispra and HPCF building. Because the HPCF building behaves almost elastic when subjected to accelerogram S7 scaled by 1.5, also the accelerogram scaled by factor 2 was used. Selected results of

time-history analyses are shown in Figures 13-15. In

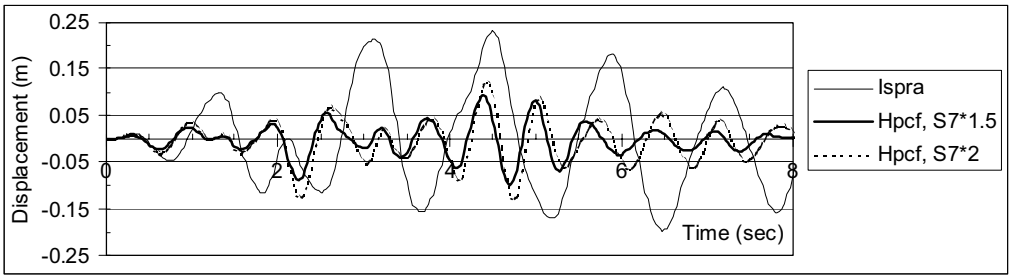

Figure 13. Top displacement time history.

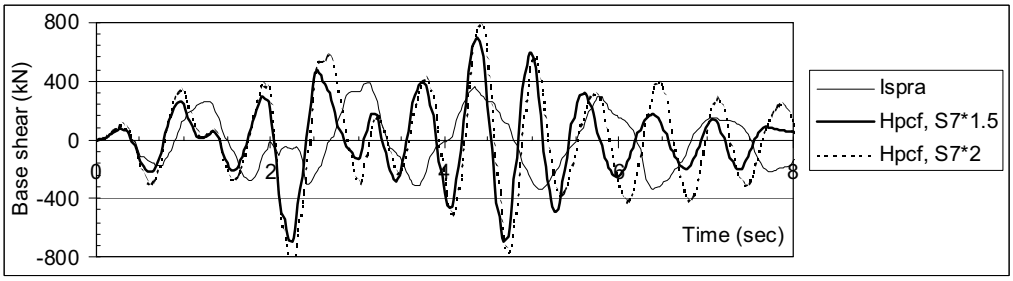

Figure 14. Base shear time history.

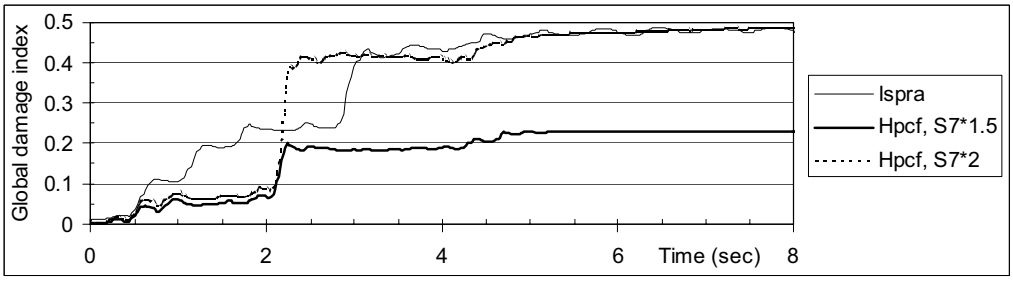

Figure 15. Global damage index time history.

Figures 13 and 14 the time histories of top displacements and base shear are presented for both investigated buildings. It can be seen from the Figures 13 and 14 that the displacements of HPCF building are substantially smaller than that of Ispra building, even in the case of using the accelerogram S7 scaled by 2. Higher stiffness of HPCF building results in substantially higher base shear and maximum value of base shear can be up to two times bigger than for Ispra building (see scaling of accelerogram S7 by factor 2).

Figure 15 presents the global structural damage index for the direction of excitation that is calculated based on all members indices by taking a local energy-weighted average. The calculation of global damage index is a feature built in CANNY program. The dam-

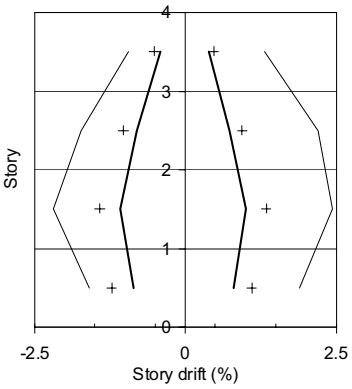

Figure 16. Envelope of story drifts for Ispra and HPCF building.

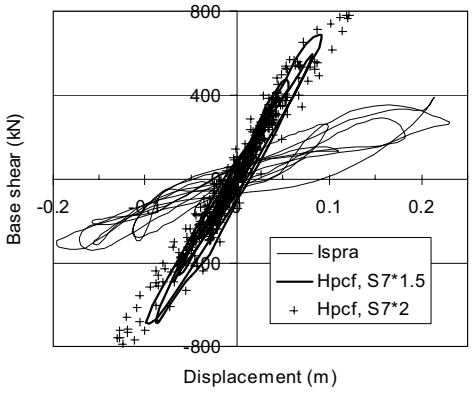

Figure 17. Base shear – top displacement relationship.

age index for each nonlinear spring is obtained by linear combination of normalized deformation and energy absorption [21]. It can be observed that the biggest amount of damage in all cases is introduced between second and third second of earthquake excitation when the final damage level is reached. It can be also seen that the global damage index of HPCF building is much smaller than that of Ispra building. In the case of scaling by factor 2, the damage of HPCF building increases to the level of damage of Ispra building.

The appropriateness of the new HPCF system can be verified also by Figure 16 which presents the envelope of story drifts for both buildings. It can be seen that the maximum story drift for Ispra building (2.5%) is reduced to approximately 1% for HPCF building.

Figure 17 shows the relation between top displacement and base shear. The indicated slopes show that HPCF building has substantially higher stiffness. It can be also seen that the hysteretic loops are much narrower for HPCF building than for Ispra building, in particular for scaling 1.5, where practically elastic behavior is obtained. Narrower hysteretic loops indicate also smaller overall damage that was already pointed out in Figure 15.

Figure 18 shows the rotation ductility factors for all investigated variants. Ductility factor is defined as a ratio between yield rotation and ultimate rotation reached during nonlinear dynamic analysis. Values equal or greater than 1.0 indicate yielding. It can be seen from Figure 18 that HPCF building has much less damage as Ispra building. As planned, the damage in HPCF building occurs only in fuses while the central part of beams in all investigated cases remains elastic. In the case of scaling by factor 2, the yielding occurs also at the bottom of columns. The fuses are specially designed to sustain higher damage and they are supposed to be replaced after an actual earthquake. More difficult is the reparation of damage at the bottom of columns which can occur during strong earthquake excitations. It is however possible to design columns to behave elastically also during stronger earthquakes.

5 Conclusions

The paper presents seismic response of a novel High Performance Composite Frame (HPCF) building system consisted of composite columns, beams and specially designed fuses that connect the two, and compares it to the response of a »classical« R/C frame building of the same dimensions. As a reference building a four-story RC frame building tested in the European Laboratory for Structural Assessment in Ispra in Italy was used.

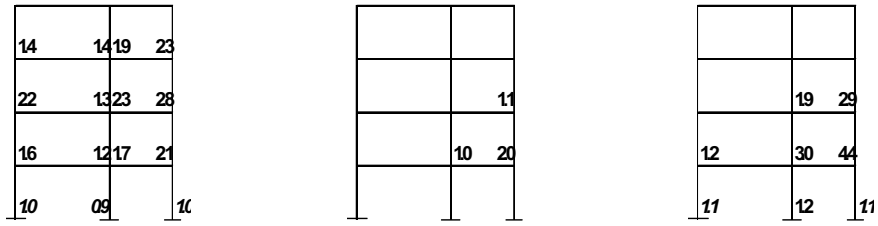

Figure 18. Rotation ductility factors for Ispra and HPCF building (outer frame). Factors equal or bigger than 1.0 indicate damage.

The analytical parameters for numerical analysis of HPCF building with nonlinear computer program CANNY-E were obtained from tests of composite members that were performed on the University of North Carolina by the second author. The mathematical modeling of nonlinear behavior of high-performance concretes is still under investigation and it is not specifically addressed in this paper. For the nonlinear analysis a three linear degrading Takeda hysteretic models adjusted to the presented experimentally obtained moment-curvature relationships were used.

One of the most important parts of the new system are specially designed fuses that connect column and beam and protect the central part of beam from damage. The special design of fuse allows higher rotational ductility factors, as they are acceptable for regular RC beams. With appropriate design is therefore possible to keep all the damage in the fuses, what simplifies the repair of building after the earthquake (precast bolted fuses are supposed to be replaced after the stronger earthquake). In order to achieve the sufficient beam protection, the stiffness, strength and the length of fuse should be carefully selected and matched with the beam span and the properties of the central part of beam. For this reason the nonlinear static analysis of an isolated HPC beam was carried out first and the most appropriate fuse/beam length ratio and fuse/beam strength ratios were determined. The analysis showed that the proposed fuse with the length equal to approximately 15% of beam span is able to protect the central part of the beam only if some additional reinforcement bars are added at the top of the fuse. This problem could be solved also with an increase of the fuse length.

In the second part of the paper the response of RC Ispra frame building and newly constructed HPCF building is compared. Good seismic properties of tested members translate to good seismic response of the HPCF building. Under the same seismic excitations the HPCF building exhibited very good seismic response. It experienced up to 50% smaller ultimate displacements, higher ultimate strength, substantially smaller story drifts and slower stiffness degradation. The damage in beams was low and concentrated in highly ductile fuse zones, while central beam regions remained elastic. In the case of original accelerogram from Ispra test, the columns remain elastic. The damage is bigger if accelerogram is scaled by factor 2. In this case the damage starts to develop also at the bottom of columns. The observed plastic mechanisms are favorable, the frames tend to develop global plastic mechanism, but even for the strongest loading used, a failure mechanism was not reached. Also the overall damage is much smaller for HPCF building what can be seen from global damage index time history.

Finally, it should be pointed out that while behavior of all frame members was experimentally evaluated, behavior of connections between these members was not tested. Instead, connections were assumed to be

"sufficiently strong" (e.g. linearly elastic) not to fail under seismic excitations. Since proper detailing of these connections and evaluation of their performance under seismic excitations was not fully addressed in the presented project, this critical issue should be explored in a greater detail in the future investigations.

It could be also concluded that the two-dimensional layout of SIMCON and its unique manufacturing properties related to its fiber-mat configuration, open up novel possibilities for a cost-effective and improved structural performance that were not previously possible using construction materials. Hence, the presented approach might provide some unique new ways of developing durable and cost-effective high-performance infrastructural systems, essential for the economic well being of a nation in this next century.

Acknowledgements

The work of the first author was partially supported by research fund of Faculty of Architecture in Ljubljana as well as by the Ministry for Science and Technology of the Republic of Slovenia. The investigation work of the second author was partially supported by NSF grants CMS-9632443 with Dr. S. C. Liu as Program Director as well as Ms. C. Dudka as International-Program Director.

REFERENCES

[1] Shah, S. July 1988. Theoretical Models for Predicting the Performance of Fiber Reinforced Concrete, Journal of Ferrocement, pp. 263-284.

[2] Naaman, A. E., Harajli, M. H. 1990. Mechanical Properties of High Performance Concretes, Report SHRP-C/WP-90-004, Strategic Highway Research Program, National Research Council.

[3] Naaman, A. E. 1992. SIFCON: Tailored Properties for Structural Performance, High Performance Fiber Reinforced Cement Composites, E & FN Spon, pp. 18-38.

[4] Hackman, L. E., Farrell, M. B., Dunham, O. O. Dec. 1992. Slurry Infiltrated Mat Concrete (SIMCON), Concrete International, pp. 53-56.

[5] Krstulovič-Opara, N., Dogan, E., Uang, C. -M, Haghayeghi, A., "Flexural Behavior of Composite R.C. - SIMCON Beams," ACI *Structural Journal*, September-October 1997, pp. 502 - 512.

[6] Krstulovič-Opara, N., Malak, S., "Micromechanical Tensile Behavior of Slurry Infiltrated Fiber Mat Concrete (SIMCON)", ACI *Materials Journal*, September - October 1997, Vol. 94, No. 5, pp. 373 - 384.

[7] Krstulovič-Opara, N., Al-Shannag, M. J., "Compressive Behavior of SIMCON," ACI *Materials Journal*, May - June 1999, pp. 367 - 377.

[8] Lankard, D. 1984. Slurry Infiltrated Fiber Concrete (SIFCON): Properties and Applications, Potential for Very High Strength Cement Based Materials, Proc. of Material Research Society, Vol. 42, pp. 277 - 286.

[9] Krstulovič-Opara, N., Al-Shannag, M. J. Jan.-Feb. 1999. Slurry Infiltrated Mat Concrete (SIMCON) - Based Shear Retrofit of Reinforced Concrete Members, ACI Structural Journal, pp. 105 - 114.

[10] Naaman, A., Wight, J., Abdou, H. November 1987. SIFCON Connections for Seismic Resistant Frames, Concrete International, pp. 34 - 38.

[11] Krstulovič-Opara, N., LaFave, J., Dogan, E., Uang, C. - M. 2000. Seismic Retrofit With Discontinuous SIMCON Jackets, HPFRC in Infrastructural Repair and Retrofit, ACI Special Publication SP-185.

[12] Dogan, E., Hill, H., Krstulovič-Opara, N. 2000. Suggested Design Guidelines for Seismic Retrofit With SIMCON & SIFCON, HPFRC in Infrastructural Repair and Retrofit, ACI SP-185.

[13] Kilar, V., Krstulovič-Opara, N. 2001. Seismic behavior of a high-performance composite frame building made with advanced cementitious composites, ISEC 2001, Hawaii, pp. 681-686.

[14] Vasconez, R. M., Naaman, A. E., Wight, J. K. 1997. Behavior of Fiber Reinforced Connections for Precast Frames Under Reversed Cyclic Loading, Report Number UMCEE 97-2, The University of Michigan.
[15] Wood, B. T., Use of Slurry Infiltrated Fiber Concrete (SIFCON) in Hinge Regions for Earthquake Resistant Concrete Moment Frames, Ph.D. Thesis, Department of Civil Engineering, North Carolina State University, 2000.
[16] Shah, S., Ahmad, S., *High Performance Concretes: Properties and Applications*, McGraw Hill, 1994.
[17] Negro, P., Verzelletti, G., Magonette, G.E. & Pinto, A.V. 1994. Tests on a Four-Storey Full-Scale R/C Frame Designed According to Eurocodes 8 and 2: Preliminary Report.
[18] Sabnis, G. M., Harris, H. G., White, R. N., and Mirza, M. S. 1983. Structural Modeling and Experimental Techniques, Civil Engineering Series, Prentice Hall, Inc., Englewood Cliffs, NJ.
[19] Li, K.N. 1997. CANNY-E. Three-dimensional nonlinear dynamic structural analysis computer program package. Canny Consultants Pte Ltd.
[20] Faella G., Kilar V., Magliulo G. 2000. Overstrength factors for 3D R/C buildings subjected to bidirectional ground motion, 12. World conference on Earthquake Engineering, Auckland, New Zealand.
[21] Park, Y.J. and Ang, A. H-S. 1985. Mechanistic Seismic Damage Model for Reinforced Concrete, Journal of Structural Engineering, ASCE, Vol. 111, No. ST4, pp. 722-739.